ARTICLE

Journal of
Sensor Science and Technology

The Korean Sensors Society

Highly Sensitive Flexible Strain Sensor Based on Laser-Induced Graphene for Wearable Applications

Yun-Jin Jeong[1], Jongsung Park[2], and Dong-Su Kim[3,+]

[1]*Department of Automatic System Engineering, Chosun College of Science & Technology, Gwangju 61453, Republic of Korea*
[2]*Department of Precision Mechanical Engineering, Kyungpook National University, Sangju, Gyeongsangbuk-do, 37224, Republic of Korea*
[3]*National Center for Nano Process & Equipments, Energy & Nano Technology Group, Korea Institute of Industrial Technology (KITECH), Gwangju 61012, Republic of Korea*

Cite This: *J. Sens. Sci. Technol. Vol. 35, No. 4 (2026) 306-312* https://doi.org/10.46670/JSST.2026.35.4.306

ABSTRACT: Flexible strain sensors have attracted increasing attention owing to their potential for wearable electronics and healthcare monitoring applications. However, complex fabrication processes, high manufacturing costs, and limited sensitivity continue to hinder their widespread practical applications. In this study, a highly sensitive and flexible strain sensor based on laser-induced graphene (LIG) was developed through a simple and cost-effective transfer process. Three-dimensional porous LIG networks were directly fabricated on polyimide (PI) films using a commercially available diode laser and subsequently embedded into a flexible polydimethylsiloxane (PDMS) matrix through casting and peel-off processes. The nine LIG-patterned areas within the 3 × 3 array exhibited consistent electrical characteristics, with an average sheet resistance of 70.13 Ω sq^{-1} and a mean standard deviation of 13.60 Ω sq^{-1}. Electromechanical characterization demonstrated outstanding strain sensitivity, achieving a maximum gauge factor (GF) exceeding 350 within a 5% strain range, together with stable and repeatable sensing performance. For wearable applications, the fabricated sensor successfully detected radial arterial pulse waves under both resting and post-exercise conditions. Furthermore, the proposed LIG sensor exhibited excellent electromechanical durability under tensile, bending, and twisting deformations, highlighting its potential for high-performance wearable electronics and stretchable electronic applications.

KEYWORDS: *Laser-induced graphene, Diode laser, Flexible strain sensor, High sensitivity, Wearable healthcare*

1. INTRODUCTION

Flexible and stretchable electronics have attracted considerable attention over the past decade owing to their wide-ranging applications in wearable healthcare, electronic skin, soft robotics, and human–machine interfaces [1-3]. Among the key functional components of these systems, flexible strain sensors capable of converting mechanical deformation into electrical signals have become indispensable for monitoring both human motion and physiological activities [2,4]. Such sensors are required to simultaneously provide excellent mechanical compliance and high electromechanical sensitivity for detecting a wide range of mechanical stimuli, from large body movements to subtle physiological signals such as respiration and arterial pulse waves [5,6]. To meet these requirements, extensive research has focused on integrating conductive nanomaterials, including graphene, carbon nanotubes, metallic nanowires, and MXenes, into flexible polymer substrates to improve sensing performance [2,3]. Although significant progress has been achieved, many reported flexible strain sensors still suffer from complicated fabrication procedures, high manufacturing costs, limited production efficiency, and insufficient mechanical stability under repeated deformation, thereby limiting their practical use in wearable sensing applications [6,7].

Laser-induced graphene (LIG) has recently emerged as a promising platform for flexible strain sensors because of its simple fabrication process, excellent electrical conductivity, and compatibility with scalable manufacturing [1,8]. LIG is directly generated by laser irradiation of polyimide (PI), producing a three-dimensional porous graphene network without requiring masks, catalysts, or chemical treatments [8].

[+]Corresponding author: dskim27@kitech.re.kr
Received : Jun. 26, 2026, Revised : Jul. 6, 2026, Accepted : Jul. 13, 2026

Compared with conventional graphene synthesis techniques, laser direct writing offers a rapid, environmentally friendly, and cost-effective approach for fabricating conductive graphene patterns [8]. Although infrared CO_2 laser systems have been widely adopted for LIG fabrication, alternative laser sources with shorter wavelengths have also been explored to improve patterning precision and expand fabrication capability [9].

Despite these advantages, the porous LIG network directly formed on PI substrates remains mechanically fragile and is susceptible to cracking or delamination under repeated mechanical deformation [10]. Consequently, transferring the LIG network into an elastomeric substrate is an effective strategy for enhancing its mechanical robustness while preserving its electrical characteristics. Among various elastomeric materials, polydimethylsiloxane (PDMS) has been widely employed because of its excellent flexibility, biocompatibility, and ease of processing. Previous studies have demonstrated that embedding porous LIG within a PDMS matrix through casting and transfer processes effectively enhances structural integrity while maintaining the intrinsic electrical properties of the graphene network [10-12]. Nevertheless, simultaneously achieving high sensitivity, stable electrical performance, and reliable operation under low-strain deformation remains challenging in wearable strain-sensing applications [7].

In this study, a highly sensitive flexible strain sensor based on LIG was fabricated using a commercial diode laser and a simple casting and peel-off transfer process. The porous LIG network was successfully embedded into a PDMS matrix to improve its mechanical robustness and flexibility. The LIG-patterned areas within the 3 × 3 array exhibited consistent electrical characteristics, with an average sheet resistance of 70.13 Ω sq^{-1} and a mean standard deviation of 13.60 Ω sq^{-1}, while the fabricated sensor achieved a maximum gauge factor (GF) exceeding 350 within a strain range of 5%. In addition, stable and repeatable sensing responses were obtained under cyclic tensile loading. Furthermore, the proposed LIG structure was demonstrated as a stretchable conductive interconnect capable of maintaining stable electrical operation during bending and twisting. Finally, to demonstrate its practical applicability for wearable healthcare, the fabricated sensor was employed for real-time monitoring of human wrist arterial pulse waves under both resting and post-exercise conditions, demonstrating its potential for wearable physiological monitoring and next-generation flexible electronic systems.

2. EXPERIMENTAL

2.1 Fabrication of Flexible LIG Strain Sensor

The overall fabrication procedure of the flexible LIG/PDMS strain sensor is illustrated in Fig. 1. The sensor consists of a porous LIG sensing layer embedded within a flexible PDMS substrate, as shown in Fig. 1(a). A commercial 25-μm-thick PI

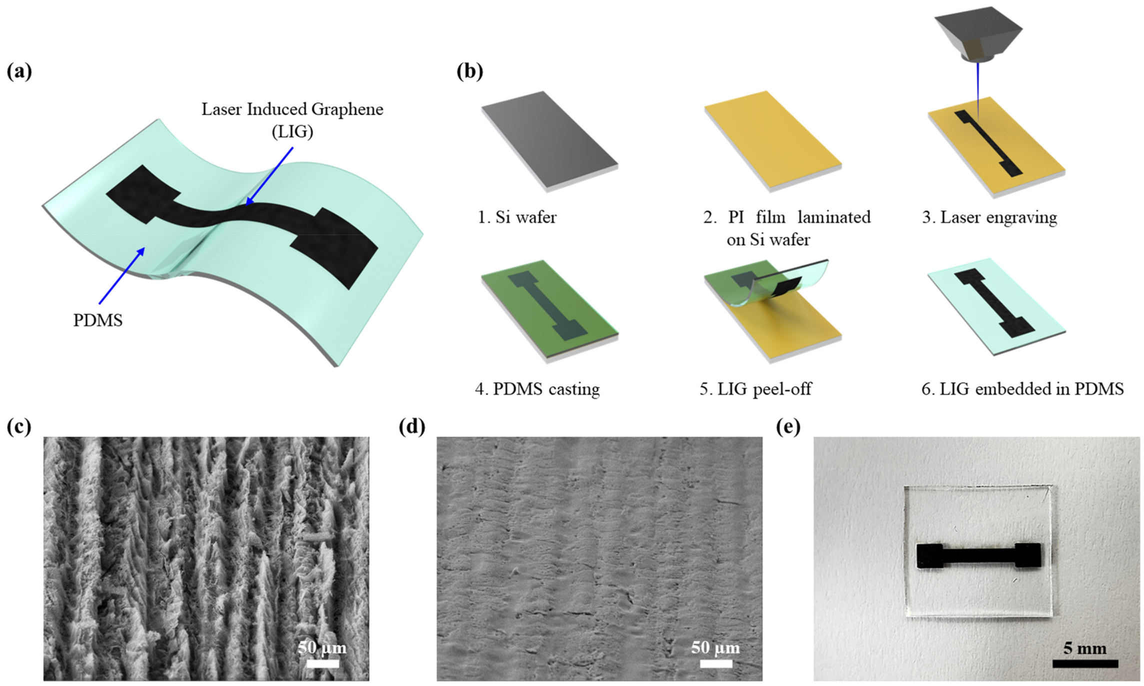

Fig. 1. (a) Schematic illustration of the flexible LIG/PDMS strain sensor. (b) Step-by-step fabrication process involving PI lamination on a Si wafer, laser engraving, PDMS casting, and peel-off. SEM images of (c) the laser-induced graphene (LIG) surface showing a 3D porous network and (d) the transferred LIG embedded in PDMS. (e) Optical photograph of the fabricated flexible strain sensor.

film was first laminated onto a cleaned 4-inch silicon (Si) wafer using a vacuum laminator to provide a flat and stable surface for laser processing. Conductive LIG patterns were directly fabricated using a commercial laser engraving system equipped with a continuous-wave (CW) blue diode laser (450 nm, maximum output power of 10 W). The laser processing parameters were set to a laser power of 3.5 W, a scanning speed of 200 mm s^{-1}, and a hatch spacing of 50 μm. The detailed fabrication procedure, including PI lamination, laser engraving, PDMS casting, and peel-off transfer, is presented in Fig. 1(b).

Following laser irradiation, PDMS (Sylgard 184, Dow Corning, USA) base and curing agent were mixed at a weight ratio of 10:1, degassed under vacuum for approximately 30 min, and cast onto the laser-patterned PI substrate using a doctor blade to form a uniform encapsulation layer. The sample was subsequently cured at 80°C for 2 h. After curing, the PDMS layer was carefully peeled from the PI substrate, thereby transferring and embedding the porous LIG network into the flexible PDMS matrix. The transferred LIG embedded in the PDMS substrate and the completed flexible strain sensor are shown in Fig. 1(d) and (e), respectively. Finally, copper wires were attached to both ends of the transferred LIG electrodes using conductive silver paste to establish reliable electrical connections.

2.2 Morphological and Electrical Characterization

The morphology of the fabricated LIG was characterized using field-emission scanning electron microscopy (FE-SEM) to investigate the three-dimensional porous graphene network generated by laser-induced carbonization. Representative FE-SEM images of the fabricated LIG are presented in Fig. 1(c).

To evaluate the electrical uniformity of the fabricated LIG patterns, a 3 × 3 sensor array was fabricated on a 4-inch PI substrate, as shown in Fig. 2(a). The sheet resistance (R_s) distribution was measured using a non-contact sheet resistance mapping system (EddyCus TF map 2530, SURAGUS GmbH, Germany), which employs a high-frequency eddy-current sensing technique for non-destructive electrical characterization. The corresponding sheet resistance mapping is presented in Fig. 2(b). The sheet resistance statistics were determined using

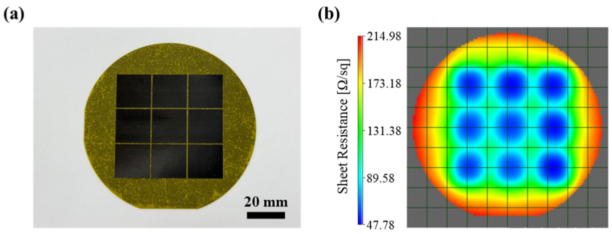

Fig. 2. (a) Optical image of the 3 × 3 LIG-patterned array fabricated on a 4-inch PI substrate. (b) Sheet resistance mapping profile of the nine LIG-patterned areas within the 3 × 3 array.

Table 1. Sheet resistance characteristics of the fabricated LIG.

Parameter	Value
Measurement area	LIG-patterned areas
Minimum sheet resistance (Ω sq^{-1})	47.78
Maximum sheet resistance (Ω sq^{-1})	126.94
Average sheet resistance (Ω sq^{-1})	70.13
Standard deviation (Ω sq^{-1})	13.60

the nine LIG-patterned areas within the 3 × 3 array while excluding the surrounding bare PI regions. The minimum, maximum, average, and mean standard deviation of the measured sheet resistance are summarized in Table 1.

2.3 Electromechanical Characterization

The electromechanical performance of the fabricated LIG/PDMS strain sensor was evaluated using a universal testing machine (EZ-L, Shimadzu Corporation, Kyoto, Japan), while the corresponding electrical resistance was simultaneously monitored using a digital multimeter (USB-4065, National Instruments, Austin, TX, USA). Uniaxial tensile strains ranging from 1% to 5% were sequentially applied at a constant crosshead speed of 1 mm min^{-1}.

The relative resistance change ($\Delta R/R_0$) was calculated according to Eq. (1), where R_0 and R represent the initial resistance and the measured resistance under the applied strain, respectively.

$$\frac{\Delta R}{R_0} = \frac{(R-R_0)}{R_0} \tag{1}$$

The GF, which represents the strain sensitivity of the sensor, was calculated according to Eq. (2), where ε is the applied tensile strain.

$$GF = \frac{\Delta R/R_0}{\varepsilon} \tag{2}$$

2.4 Demonstration of Stretchable LIG Interconnect

To evaluate the electromechanical stability of the fabricated LIG as a stretchable conductor, a serpentine-patterned LIG interconnect integrated with a commercial blue light-emitting diode (LED) was fabricated. The electrical functionality of the device was examined under tensile, bending, and twisting deformations by monitoring the LED operation. This demonstration was performed to verify the electrical continuity and mechanical reliability of the LIG interconnect under various mechanical deformation modes.

2.5 Wearable Pulse Monitoring

To evaluate the wearable pulse monitoring capability of the fabricated sensor, the strain sensor was attached over the radial artery of the wrist using a transparent medical dressing film (Tegaderm™, 3M, St. Paul, MN, USA). The resistance variation generated by arterial expansion during the cardiac cycle was continuously recorded under resting and post-exercise conditions. The acquired resistance signals were converted into normalized $\Delta R/R_0$ and processed for pulse waveform analysis.

3. RESULTS AND DISCUSSIONS

3.1 Sheet Resistance Distribution of the Wafer-Scale LIG Array

The electrical characteristics of the fabricated LIG were evaluated using the nine patterned areas within a wafer-scale 3 × 3 array. The 3 × 3 array of LIG patterns was successfully fabricated over a 4-inch PI substrate without noticeable macroscopic defects or discontinuities, as shown in Fig. 2(a). The corresponding sheet resistance distribution was quantitatively characterized using a non-contact eddy-current mapping system, as shown in Fig. 2(b). The sheet resistance statistics were obtained exclusively from the nine LIG-patterned areas, excluding the surrounding bare PI regions. As summarized in Table 1, the minimum and maximum sheet resistance values were 47.78 and 126.94 Ω sq^{-1}, respectively. The average sheet resistance was 70.13 Ω sq^{-1}, with a mean standard deviation of 13.60 Ω sq^{-1}. These results indicate that the diode laser process produced LIG patterns with relatively consistent electrical characteristics across the wafer-scale 3 × 3 array. The observed consistency supports the reproducibility of the fabrication process for producing multiple flexible sensing elements on a single substrate.

3.2 Electromechanical Performance of the LIG/PDMS Strain Sensor

The electromechanical characteristics of the transferred LIG/PDMS strain sensor were systematically investigated under tensile deformation. The baseline resistance was continuously monitored for 1800 s without external loading, exhibiting negligible electrical drift and stable signal output, as shown in Fig. 3. This baseline stability indicates that the resistance signal remained relatively insensitive to time-dependent fluctuations under static conditions. The baseline stability also provided a reliable reference for distinguishing the resistance changes induced by subsequent tensile deformation.

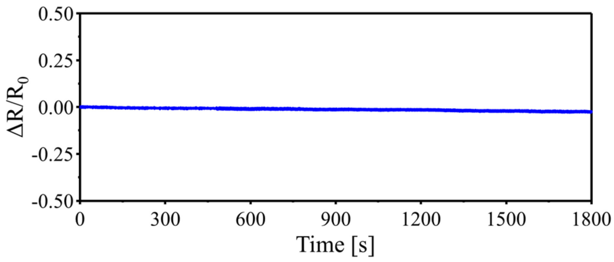

Fig. 3. Baseline electrical stability of the fabricated LIG/PDMS strain sensor measured for 1800 s without external tensile loading.

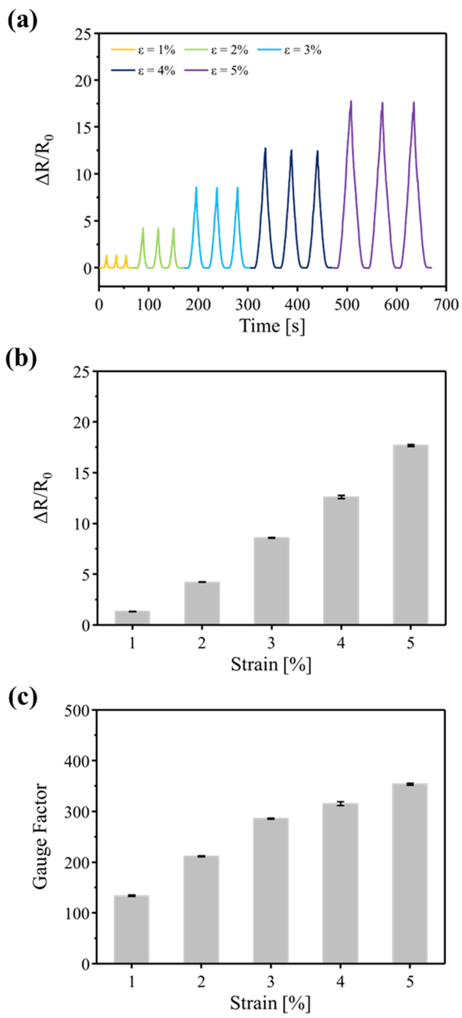

Fig. 4. Electromechanical performance of the LIG/PDMS strain sensor. (a) Dynamic relative resistance responses under repeated tensile strains ranging from 1% to 5%, (b) $\Delta R/R_0$ as a function of applied strain, and (c) GF as a function of applied strain.

The dynamic relative resistance responses under repeated tensile strains ranging from 1% to 5% are presented in Fig. 4(a). Distinct and reproducible resistance peaks were observed for each applied strain, indicating stable sensing behavior with good repeatability. The sensing performance was quantitatively evaluated using the $\Delta R/R_0$ and the corresponding GF. The $\Delta R/R_0$ increased monotonically with increasing tensile strain, reaching approximately 17.6 at 5% strain, as shown in Fig. 4(b). The corresponding GF also increased with applied strain and exceeded 350 at 5% strain, demonstrating high sensitivity within a relatively small deformation range, as shown in Fig. 4(c).

The high sensitivity is attributed to the conductive porous graphene network embedded within the PDMS matrix. During tensile deformation, separation between adjacent graphitic domains increases both the tunneling distance and contact resistance, resulting in a significant increase in the overall electrical resistance. Upon release of the applied strain, the elastic recovery of the PDMS matrix facilitates partial reconstruction of the conductive pathways, allowing the sensor resistance to recover toward its initial value. However, complete baseline recovery was not achieved after unloading, and a residual baseline shift remained, which may be associated with partial irreversible rearrangement of the porous LIG network. The magnitude of this baseline shift corresponded to approximately 1.13% of the maximum sensor response, indicating a relatively limited influence on the full-scale output. Although a residual baseline offset remained, the resistance peaks at each applied strain were clearly distinguishable and repeatable.

3.3 Stretchable LIG Interconnect Demonstration

Beyond strain sensing, the fabricated LIG structures were further evaluated as stretchable conductive interconnects. A serpentine-patterned LIG electrode integrated with a blue LED was fabricated to visually demonstrate its electromechanical response. In the initial state, the LED exhibited stable illumination, confirming reliable electrical conduction through the LIG interconnect, as shown in Fig. 5(a). When tensile deformation was applied, the LED brightness noticeably decreased because of the increase in electrical resistance caused by stretching of the serpentine LIG pathway, as shown in Fig. 5(b). This behavior clearly demonstrates the strain-dependent electrical characteristics of the fabricated LIG structure.

The serpentine geometry accommodated the applied tensile deformation through changes in the curvature and spacing of the conductive pathway. The increase in resistance during stretching may be attributed to partial separation and rearrangement of the porous LIG network, which reduced the current supplied to the LED. Therefore, the change in LED illumination provided a direct visual measure of the resistance modulation induced by tensile deformation. These observations indicate that the patterned LIG structure can function as both a mechanically compliant interconnect and a strain-responsive conductive element.

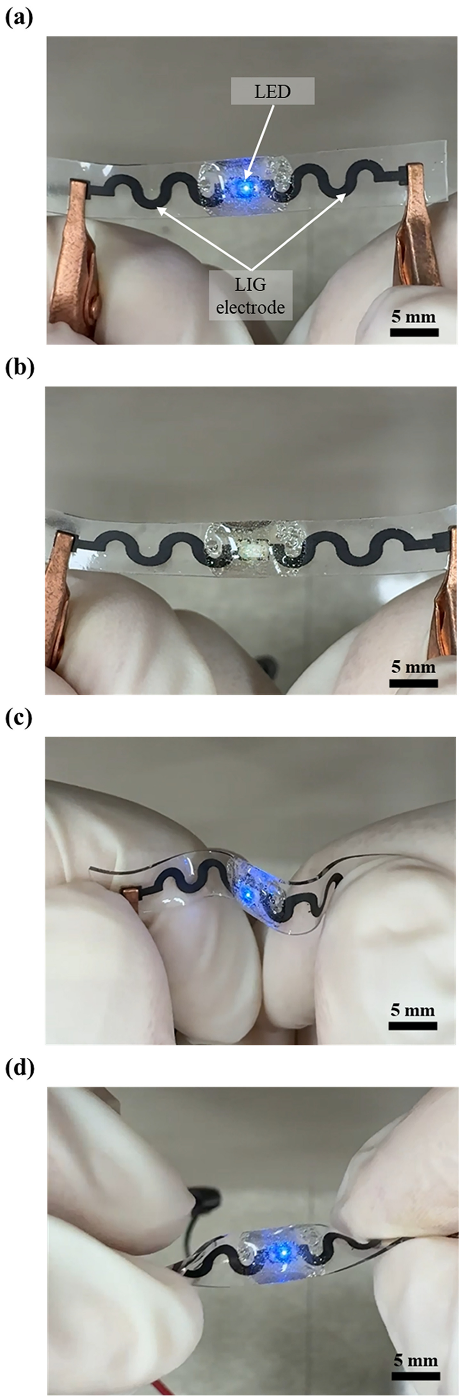

Fig. 5. Optical photographs demonstrating the electromechanical durability and switching behavior of the serpentine LIG interconnect integrated with a blue LED under various mechanical deformations. (a) Pristine state with a turned-on LED, (b) stretched state showing the turned-off LED due to the strain-induced resistance increase, (c) bending, and (d) twisting.

In contrast to its response under tensile deformation, the LED maintained stable illumination without noticeable flickering or electrical interruption during bending and twisting, as shown in Fig. 5(c) and (d), respectively. This result indicates that the serpentine geometry effectively accommodated complex mechanical deformation while preserving electrical continuity. The demonstrated electromechanical stability suggests that the proposed LIG structure can serve not only as a highly sensitive strain-sensing element but also as a reliable stretchable interconnect for flexible electronic systems.

3.4 Wearable Pulse Monitoring

To verify the practical applicability of the developed strain sensor for wearable healthcare, real-time wrist pulse monitoring was performed by attaching the flexible sensor directly over the radial artery, as shown in Fig. 6(a). The sensor was secured using a transparent medical dressing film, while the electro-pads provided stable electrical connections during the measurement. Owing to the mechanical flexibility and conformability of the LIG/PDMS structure, the sensing region maintained close contact with the skin and followed the small surface deformations induced by arterial pulsation.

Representative pulse waveforms recorded under resting and post-exercise conditions are presented in Fig. 6(b) and (c), respectively. Under the resting condition, periodic pulse signals with relatively stable amplitudes and intervals were clearly detected, yielding an average heart rate of 72 bpm and a normalized signal amplitude of 0.0228 ± 0.0098. The periodic resistance variation indicates that the sensor was sufficiently sensitive to detect the subtle expansion and contraction of the radial artery during each cardiac cycle. Following physical exercise, the pulse interval became noticeably shorter, corresponding to an increased heart rate of 84 bpm, while the normalized pulse amplitude increased to 0.0894 ± 0.0161. Compared with the resting state, the heart rate increased by approximately 16.7%, and the normalized pulse amplitude increased by approximately 3.9 times. These changes reflect the enhanced cardiovascular activity induced by exercise, which produces more frequent and pronounced arterial deformation at the wrist. The clear differences between the resting and post-exercise pulse waveforms demonstrate that the fabricated sensor can distinguish variations in both pulse frequency and signal amplitude under different physiological conditions. The periodic pulse signals were consistently detected under both conditions, confirming that the sensor maintained reliable skin contact and stable signal acquisition during the measurements. These results confirm that the combination of high electromechanical sensitivity, mechanical compliance, and conformal skin contact enables the LIG/PDMS strain sensor to detect weak physiological signals in real time. The ability to distinguish resting and post-exercise pulse characteristics highlights its potential for wearable heart-rate monitoring, exercise-state assessment, and continuous personalized healthcare applications.

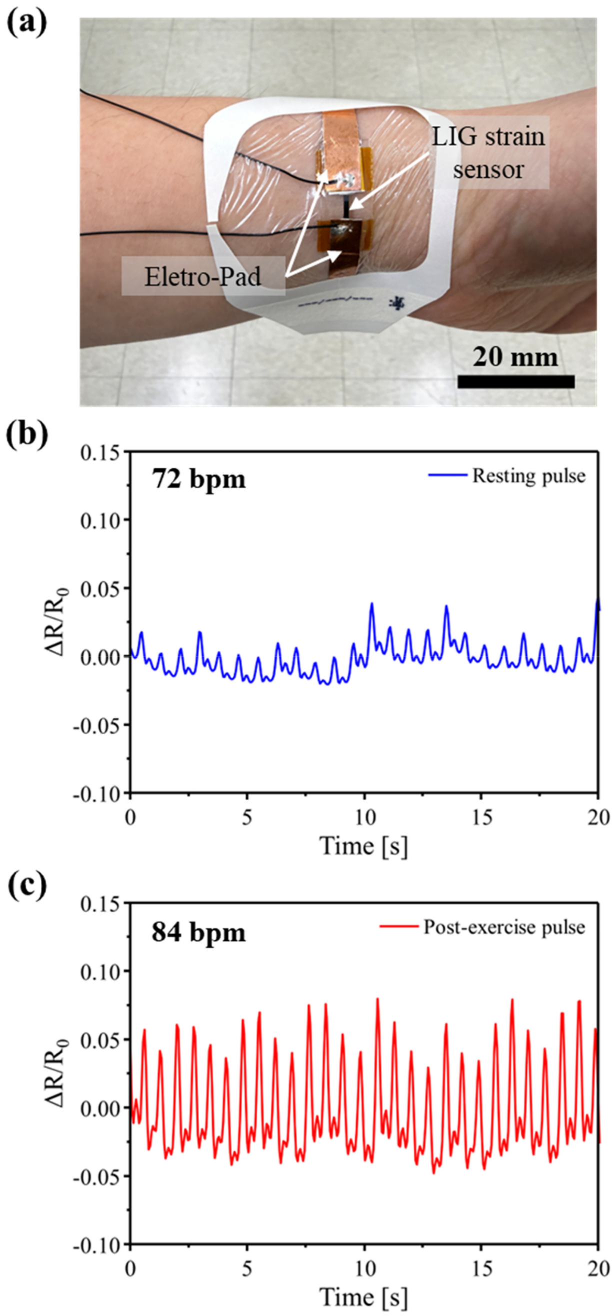

Fig. 6. Wearable health monitoring applications. (a) Photograph of the LIG strain sensor attached to a human wrist. Real-time relative resistance response capturing the arterial pulse waves under (b) resting and (c) post-exercise conditions.

4. CONCLUSIONS

A highly sensitive and flexible strain sensor based on a three-dimensional (3D) porous LIG network embedded within a PDMS matrix was successfully developed. A commercial diode laser direct-writing system was used to fabricate a 3 × 3 LIG-patterned array with consistent electrical characteristics, resulting in an average sheet resistance of 70.13 Ω sq^{-1} and a mean standard deviation of 13.60 Ω sq^{-1} across the LIG-patterned areas. The fabricated sensor exhibited high electromechanical sensitivity, achieving a maximum GF exceeding 350 within a strain range of 5%, together with stable and repeatable sensing responses under cyclic tensile loading. Furthermore, a serpentine-patterned LIG structure successfully functioned as a stretchable conductive interconnect, maintaining stable electrical operation under bending and twisting deformation while exhibiting controllable resistance variation during tensile loading. The high sensitivity of the proposed sensor also enabled reliable detection of subtle biomechanical deformation, as demonstrated by real-time monitoring of human wrist arterial pulse waveforms under both resting and post-exercise conditions. Overall, the proposed LIG/PDMS platform combines scalable fabrication, mechanical flexibility, and high sensing performance, demonstrating its potential for wearable physiological monitoring, stretchable interconnects, flexible electronic systems, and electronic skin applications.

CRediT Authorship Contribution Statement

Yun-Jin Jeong: Methodology, Resources, Supervision, Validation, Writing – review & editing. **Jongsung Park:** Formal analysis, Investigation, Validation. **Dong-Su Kim:** Conceptualization, Data curation, Formal analysis, Funding acquisition, Investigation, Methodology, Project administration, Resources, Validation, Visualization, Writing – original draft, Writing – review & editing.

Declaration of Competing Interest

The authors declare that they have no competing financial interests or personal relationships that may have influenced the work reported in this paper.

Acknowledgements

This work was supported by the National Research Foundation of Korea (NRF) grant funded by the Korean government (MSIT) (RS-2022-NR072456).

REFERENCES

[1] P. Chen, J. Yang, Z. Xu, J. Zhang, Z. Wang, J. Huang, et al., Laser-induced graphene for pressure and strain sensors: Fabrication, performance optimization, and applications, Small (2026) e2513163.

[2] J. Zhu, X. Huang, W. Song, Physical and chemical sensors on the basis of laser-induced graphene: Mechanisms, applications, and perspectives, ACS Nano 15 (2021) 18708–18741.

[3] I.J. Oh, D. Kim, S.-Y. Kim, S. Choi, W.-H. Yeo, H.-R. Lim, Advances in laser-induced graphene: Materials, fabrication, and emerging applications in flexible electronics, Front. Nanotechnol. 7 (2025) 1750193.

[4] Y.-H. Yen, C.-S. Hsu, Z.-Y. Lei, H.-J. Wang, C.-Y. Su, C.-L. Dai, et al., Laser-induced graphene stretchable strain sensor with vertical and parallel patterns, Micromachines 13 (2022) 1220.

[5] H. Yoon, K. Lee, H. Shin, S. Jeong, Y.J. Lee, S. Yang, et al., In situ co-transformation of reduced graphene oxide embedded in laser-induced graphene and full-range on-body strain sensor, Adv. Funct. Mater. 33 (2023) 2300322.

[6] T. Raza, M.K. Tufail, A. Ali, A. Boakye, X. Qi, Y. Ma, et al., Wearable and flexible multifunctional sensor based on laser-induced graphene for the sports monitoring system, ACS Appl. Mater. Interfaces 14 (2022) 54170–54181.

[7] S. Sadeghzadeh, Highly sensitive strain sensors with minimal hysteresis using laser-induced graphene, Appl. Phys. A 131 (2025) 293.

[8] R. Ye, D.K. James, J.M. Tour, Laser-induced graphene, Acc. Chem. Res. 51 (2018) 1609–1620.

[9] A.F. Carvalho, A.J.S. Fernandes, C. Leitão, J. Deuermeier, A.C. Marques, R. Martins, et al., Laser-induced graphene strain sensors produced by ultraviolet irradiation of polyimide, Adv. Funct. Mater. 28 (2018) 1805271.

[10] A.M. Barja, Y.K. Ryu, S. Tarancón, E. Tejado, A. Hamada, A. Velasco, et al., Laser-induced graphene strain sensors for body movement monitoring, ACS Omega 9 (2024) 38359–38370.

[11] T. Jacquin, S. Wanstall, I. Park, A.A. Stokes, H. Heidari, T. Lim, et al., Wearable, near temperature insensitive laser-induced graphene nanocomposite strain sensors, J. Mater. Chem. C 13 (2025) 20000–20012.

[12] W. Wang, L. Lu, Z. Li, L. Lin, Z. Liang, X. Lu, et al., Fingerprint-inspired strain sensor with balanced sensitivity and strain range using laser-induced graphene, ACS Appl. Mater. Interfaces 14 (2021) 1315–1325.